Role of free F⁻ anions in the electrorefining of titanium in molten alkali halide mixtures

N. ENE, S. ZUCA

Romanian Academy – Institute of Physical Chemistry, Splaiul Independentei 202, Bucharest, Romania

The influence of the F/Cl atomic ratio on the morphology of titanium metal, deposited by electro-refining in various alkali halide solvent mixtures and K_2TiF_6 solute, was investigated. A continuous transition from powdery deposits in chloride mixtures (F/Cl = 0), through dendritic deposits in chloride–fluoride mixtures ($0 < $ C/Cl $ < \infty$), to coherent and adherent deposits in fluoride mixtures (F/Cl = ∞), was evidenced. This dependence was explained in terms of the increase of the thermo-dynamic stability of TiF_6^{3-} anion (and the consequent decrease of the activity of Ti^{3+}, i.e. electro-crystallization centres available in the melt), with increase of the parameter F/Cl. This is supported by the observed increase in the decomposition potential, E_d, and the shift of the Ti^{3+} discharge potential, E_p, toward more negative values, in the same sequence. The influence of the F/Cl atomic ratio on current efficiency, η, on the grain size distribution and on the chemical purity of electrodeposited titanium metallic powder, was also discussed.

List of symbols

cd	current density	$(E_{1/2})_c$	half wave potential of the complex
E_d	decomposition potential	$(E_{1/2})_f$	half wave potential of the free ion
E_p	discharge potential	η	current efficiency
		d_m	average diameter
		P_m	molar polarizing strength

1. Introduction

Interest in the electrochemistry of fluoride and fluoride–chloride solvent mixtures with K_2TiF_6 as solute has increased recently, mainly because the cathodic process is simpler. It consists of two reduction steps in fluoride solvent [1–5]:

$$TiF_6^{2-} + e^- \longrightarrow TiF_6^{3-} \qquad (1)$$

$$TiF_6^{3-} + 3e^- \longrightarrow Ti + 6F^- \qquad (2)$$
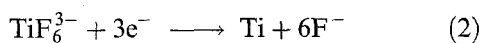
and one step, the second, in the fluoride–chloride melts [6–8]. It was also established that, in the presence of titanium metal, the K_2TiF_6 salt is reduced to the trivalent state by the following reaction:

$$3TiF_6^{2-} + Ti + 6F^- \longrightarrow 4TiF_6^{3-} \qquad (3)$$
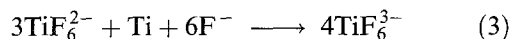
which always precedes the production of titanium metal by electrolysis [7–9].

Taking account of these findings, K_2TiF_6 was chosen as solute in the present study on titanium electrorefining in molten alkali halide mixtures. Because the anode of the electrorefining cell consists of titanium metal, (different scraps), whose presence in the electrolyte promotes the chemical reduction of K_2TiF_6 solute (Equation 3), it is obvious that the titanium cathodic reduction occurs in one step with three electron exchange regardless of the alkali halide

mixture used. Moreover, in previous works [10–12], it was shown that titanium electrorefining takes place in better conditions than classical electrolysis, because the complicating factors, such as depletion of titanium from the melt and anode gas evolution with the related technical problems of separating the anode from the cathode space are avoided; consequently both the electrolysis cell and its operation are simpler and render experimental investigation more convenient. It was also shown that the morphology of the cathodic deposit is mainly determined by the concentration of free F⁻ anions in the melt, defined by the F/Cl atomic ratio.

To confirm the decisive role played by the parameter F/Cl in controlling the electrorefining process, we also present additional data regarding its influence on the electrochemical parameters, E_d and E_p, on the current efficiency, the morphology and the chemical purity of the electrodeposited titanium.

2. Experimental details

The alkali halides employed were p.a. reagent grade. Stoichiometric K_2TiF_6 was prepared by a method described elsewhere [13] and was dried over P_2O_5 in a desiccator for several days. Special precautions were taken in preparing the melts, to remove traces of water and/or hydrolysis products. Traditional techniques, such as bubbling through the melt either argon gas saturated with CCl_4 or gaseous HCl, or

heating under vacuum by gradually increasing the temperature to the working temperature, were used.

An insulated central stainless steel (V4A extra) rod served as cathode. Cells of variable diameter, (max. content of 2000 g electrolyte) were also made of stainless steel (V4A extra) and were accommodated in an air-tight stainless steel vessel provided to operate in vacuum or controlled inert atmosphere (argon with oxygen, nitrogen and moisture content less than 15 p.p.m.). A detailed description of the electrorefining cell assembly and its operation was given previously [10–12]. All electrorefining experiments were conducted in galvanostatic conditions at a current density of $0.8 \, A \, cm^{-2}$, a constant temperature of $1023 \pm 5 \, K$ and a constant content of 10 wt % K_2TiF_6. After recovery, samples of electrodeposited titanium powder were analysed for chemical purity and their structural characteristics were determined by optical and scanning electron microscopy. The various fractions of titanium powder deposit were separated with a DIN 4180 standard sieve set. The current efficiency during electrorefining was determined by means of a copper coulometer.

Steady-state measurements were carried out at galvanostatic conditions to determine the decomposition potential, E_d, of K_2TiF_6 solute. The anode–cathode polarization curves were recorded by stepwise current increase (steps of 0.1 A) in the $0.01–3 \, A \, cm^{-2}$ range. Correction was made for ohmic voltage drop, measured by the current switch off method. Nickel wires and spectral graphite rods in a platinum crucible ($\phi = 40 \, mm$, $l = 50 \, mm$) were used as cathode and anode, respectively.

Voltammetric investigations were performed using the same container and working electrodes. The reference was a calibrated Ag/Ag^+ electrode. Use

was made of a Tacussel PRT 10-20X potentiostat driven by an IEMI–E0205 signal generator and of a LY-1600, X–Y recorder. Details of the experimental procedure are described in [12].

3. Results and discussions

3.1. Influence of the F/Cl atomic ratio on the electrodeposited titanium

The solvent salt mixtures employed in the study are listed in Table 1 along with the morphology of deposited titanium metal (4th column). Table 1 shows that two representative types of cathodic deposits were obtained in the solvent mixtures investigated: either coherent dense and adherent or metallic grains of different size and structure. As shown in Figs 1–3, regardless of the nature of the solvent salt mixture, the titanium crystals were always formed through a layer growth mechanism. However, according to the data in Table 1, the arrangement of these layers in the final structure was directly determined by the F/Cl atomic ratio (listed in the 2nd column). The experiments, carried out with equimolecular NaCl–KCl in which variable amounts of NaF were added, show that by a systematic increase of the parameter F/Cl a continuous transition occurs from what (in terms of electrocrystallization theory [14]) is called. F.I. type crystals (field oriented isolated type crystal, as in Fig. 4) to F.T. type deposits, (field oriented texture type as in Fig. 5). According to theory [14] the latter type of deposit is favoured by the presence of inhibitors at higher concentrations. Therefore the hypothesis was advanced that F^- anions act as inhibitor, most probably through two mechanisms: either physical adsorption on the active zones of crystal growth or

Table 1. F/Cl, P_m parameters and morphology of titanium cathodic deposits in various solvent mixtures

Solvent type	Composition/mol %	F/Cl*	P_m	Morphology of cathodic deposit[†]
Chlorides	LiCl 100	0	2.778	needle like crystals of different cross sections
	NaCl–KCl 50:50	0	0.836	amorophous powder
Chlorides-fluorides	NaCl–KCl–NaF 47.9:47.9:4.2	0.008	0.848	microdendrites
	NaCl–KCl–NaF 46.4:46.4:7.2	0.041	0.856	well shaped dendrites
	NaCl–KCl–NaF 43.1:43.1:13.8	0.085	0.874	dendrites with principal and secondary directions of growth
	NaCl–KCl–NaF 40.4:40.4:19.2	0.126	0.889	interpenetration of dendrites in texture type structure
Fluorides	LiF–NaF 60:40	∞	2.101	bright, compact, adherent deposit
	LiF–NaF–KF 46.4:11.6:42	∞	1.856	

* F^- anions bonded in TiF_6^{3-} complex anion are not considered.
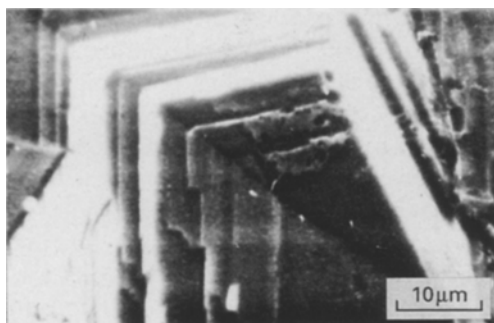[†] Analysed by scanning electron miccroscopy.

Fig. 1. 'Ridge growth' by successive layers in all fluoride solvent mixtures.

chemical stabilization of the TiF_6^{3-} complex anion, thus blocking the newly formed electrocrystallization centres, which favours the deposition shown in Fig. 5.

According to Table 1, at the two extreme values, $F/Cl = \infty$ and $F/Cl = 0$, the growth through well structured crystals ceases, and either a compact envelope $(F/Cl = \infty)$ or a powdery deposit $(F/Cl = 0)$ is obtained.

Table 1 suggests that, besides the F/Cl atomic ratio, the constituent cations of the solvent also exert an influence on the coherence of the titanium cathodic deposit. Mellors and Senderoff mentioned [15] a similar interdependence noted in other transition metals. To describe this behaviour numerous semi-quantitative relationships, involving the charge and the radius of the solvent cations, have been used. In our opinion a major role may be assigned to the ratio Z/r^2 which defines the 'polarizing strength' of a given cation. For multicomponent systems it is convenient to define a 'molar polarizing strength' which sums up the contribution of all solvent cations as follows:

$$P_m = \sum x_i \frac{Z_i}{r_i^2}$$

where x_i denotes the mole fraction of the cations and f_i and r_i the valence and crystal ionic radius, respectively. The numerical values obtained in all solvents studied are listed in the 3rd column of Table 1. As expected, in solvents containing Li^+ cation the P_m values are over three times larger than in the other solvents. In these same solvents, deposits with unusual morphology were obtained: either very large needle-like crystals of different cross sections not encountered so far [10, 14] (in LiCl solvent) or

Fig. 2. Microphotograph of titanium crystal formed at melt/gas boundary in chloride–fluoride solvent mixtures.

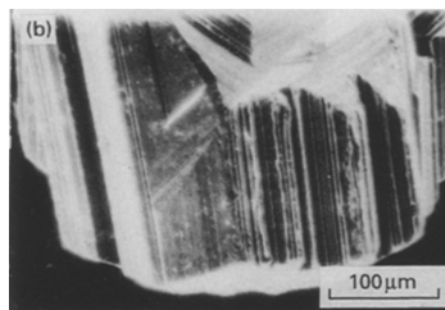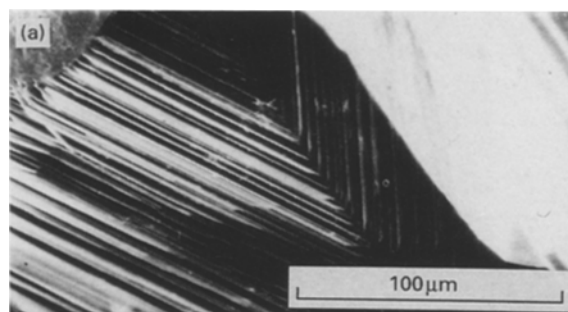

Fig. 3. Microphotograph of titanium crystal growth by completion of successive layers in different alkali halide solvents: (a) LiCl solvent; (b) NaCl–KCl–NaF solvent.

compact plating generated by a two dimensional growth (in LiF–NaF and LiF–NaF–KF solvents). According to Lumsden's anion polarization model [16], it is possible that, owing to the large 'polarizing strength' of the Li^+ ion, the ionic interactions intensify in the presence of readily polarizable TiF_6^{3-} to such an extent that the simple anion–cation associated groups are replaced by closer packed entities, which are more stable. The specificity of the cathodic deposits mentioned may be attributed to such an effect. In fact the special steric effect of the Li^+ ion, which hinders the free rotation of the nitrate ion in the $LiNO_3$ melt, is well known [17].

The influence of the F/Cl atomic ratio on the morphology of the cathodic deposit can also be explained by the thermodynamic stability of the TiF_6^{3-} ion. Although potassium hexafluorotitanate is a stable compound, its thermodynamic stability may be influenced by anions of the solvent through the following exchange reactions [18–21]:
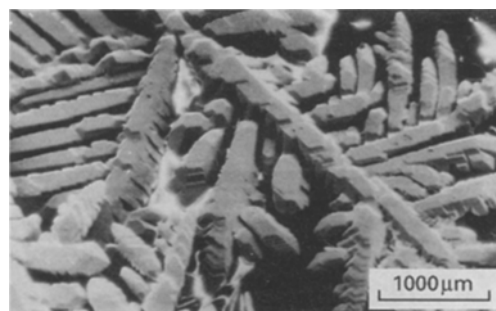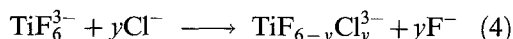
$$TiF_6^{3-} + yCl^- \longrightarrow TiF_{6-y}Cl_y^{3-} + yF^- \quad (4)$$

$$TiF_xCl_y^{(x+y-3)-} + yF^- \longrightarrow TiF_{x+y}^{(x+y-3)-} + yCl^- \quad (5)$$

Fig. 4. Dendrites with principal direction of growth in molten NaCl–KCl–5% NaF solvent mixture.
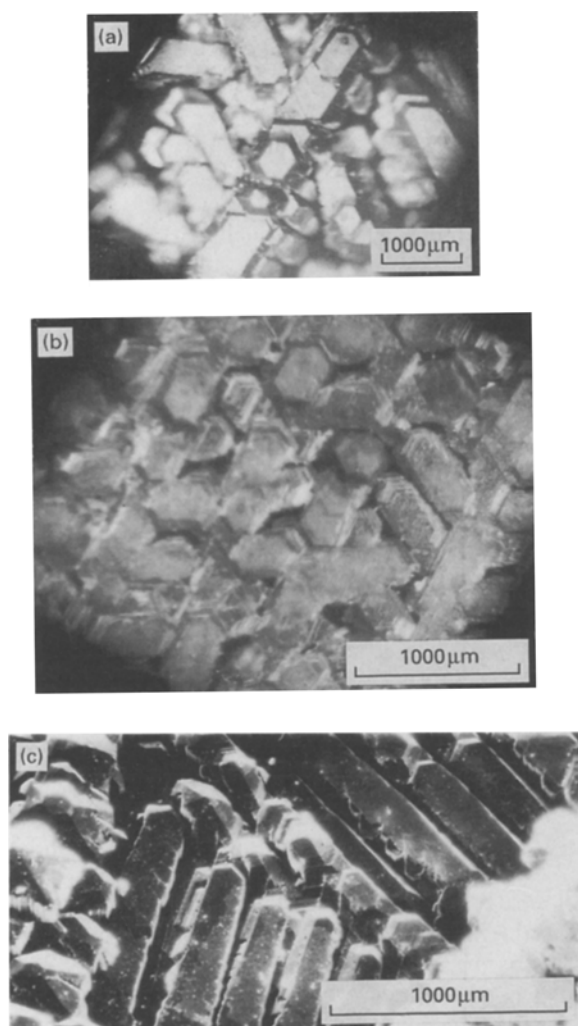
Fig. 5. Texture type deposits obtained in NaCl–KCl–15% NaF solvent mixture at different magnifications.

of which the first is considered predominant in all chloride solvents, while the second becomes more important the higher the F⁻ ion content in the electrolyte. Thus, depending on the solvent nature, the much stronger Ti–F bond is replaced by the weaker Ti–Cl bond, which brings about an increase in the activity of titanium ions in the melt and, consequently, the deposition of dendrites and powders.

Conversely, the presence of NaF represents an additional stabilizing factor; therefore the dissociation constant of TiF_6^{3-} anions and, implicitly, the number of electrocrystallization centres available, decrease with the increasing NaF content and coherent deposition is promoted.

It is obvious that such changes in the solute–solvent interaction should alter the process of titanium electroreduction. Therefore the influence of the F/Cl atomic ratio on the potassium hexafluorotitanate decomposition potential, E_d, and Ti^{3+} discharge potential, E_p, was also studied.

The polarization curves obtained with the NaCl–KCl eutectic and different additions of NaF are shown in Fig. 6. This shows a systematic increase in E_d with increasing concentration of NaF and, implicitly, the increasing F/Cl ratio take place. Thus, in the NaF-free electrolyte $E_d = 1.76\,V$ and reaches $1.83\,V$ for 15% NaF, a value which is not further changed by subsequent increase in the F⁻ concentration. According to [22], $E_d = 1.825\,V$ for single K_2TiF_6 at 1200 K.

Cyclic voltammetry shows that the increase in the parameter F/Cl is accompanied by a shift to more negative potentials of the peak corresponding to $Ti(\text{III}) \longrightarrow Ti(0)$ reduction. According to Fig. 7, the shift from the peak corresponding to NaF-free solvent mixture reaches $-0.075 \pm 0.01\,V$ when F/Cl = 0.126. This change may be associated with the formation of a mixed titanium complex $TiF_{6-y}Cl_y^{3-}$.

Heirovsky and Illkovici [23] have shown that, in the presence of a complexing agent, there is a shift of the half wave potential of the complex $(E_{1/2})_c$, with respect to the corresponding value for the discharge of the simple ion, $(E_{1/2})_f$, which is given by the following equation:

$$\Delta E_{1/2} = -\frac{RT}{nF}\ln K - \frac{RT}{nF}\ln[X^{m-}]^p \qquad (6)$$

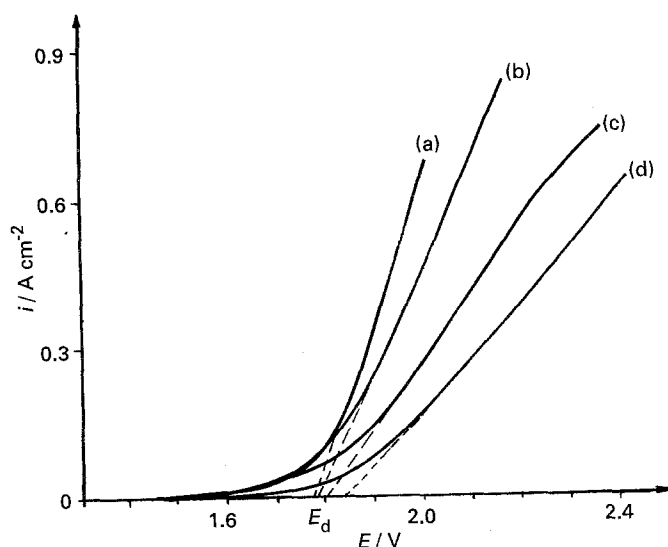where $K = [MX_p^{(mp-n)-}]/[M^{n+}][X^{m-}]^p$ and $\Delta E_{1/2} = (E_{1/2})_c - (E_{1/2})_f$.

Fig. 6. Steady-state polarization curves in molten NaCl–KCl with variable NaF addition: (a) 0, (b) 5, (c) 10 and (d) 15 wt % NaF.
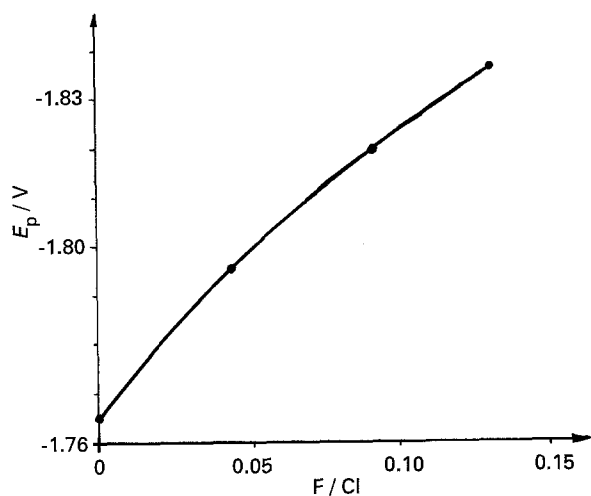
Fig. 7. E_p against the F/Cl atomic ratio in NaCl–KCl–NaF solvent mixtures.

Table 3. Oxygen and nitrogen content in different fraction of titanium powder

Solvent/mol %	Grain size distribution	Impurities/wt %	
		O_2	N_2
43.1 NaCl–43.1	0.8	0.035	0.001
KCl–13.8 NaF	0.8–0.65	0.040	0.001
	0.65–0.315	0.044	0.004
	0.315–0.100	0.050	0.004
	0.100–0.065	0.052	0.006
	< 0.065	0.066	0.007

It is obvious that $\Delta E_{1/2}$ is more negative the higher K, i.e. the more stable the complex. Consequently the data in Fig. 7 point to the increasing stability of the TiF_6^{3-}-complex with increasing concentration of F⁻ in the electrolyte.

A similar behaviour was mentioned recently [24] for the system NaCl–KCl–NaF–TiCl₃. Besides the E_p shift towards more negative values, modification of the Ti(III) reduction mechanisms induced by the increase of [Ti]/[F] ratio was also attributed to changes in the stability of $TiCl_6^{3-}$ complex.

There is no doubt that the relationship shown in Figs 6 and 7 may be regarded as additional evidence for the influence of F⁻ free ions on the thermodynamic stability of the TiF_6^{3-} ion with its implications for the morphological changes in the electrodeposition of titanium listed in Table 1.

3.2. Influence of F/Cl ratio on grain size distribution and chemical purity of titanium powder

The average diameter, d_m, of the metallic powder grains may be described [14] by the equation

$$d_m = \frac{a_1 p_1 + a_2 p_2 + \cdots + a_n p_n}{p_1 + p_2 + \cdots + p_n} \qquad (7)$$

where $a_1 \ldots a_n$ denote the sieve mesh and $p_1 \ldots p_n$

Table 2. Influence of the F/Cl atomic ratio upon d_m at different current densities in molten NaCl–KCl–NaF solvent mixtures

cd/A m⁻²	0.5×10^4	1×10^4	2×10^4
F/Cl		d_m/mm	
0	0.316	0.212	0.142
0.008	0.324	0.236	0.160
0.041	0.340	0.248	0.173
0.085	0.356	0.252	0.188
0.126	0.396	0.300	—
0.169	0.464	0.320	0.206

the weights of various grain size fractions. Table 2 lists the d_m values of the deposits recovered from molten NaCl–KCl–NaF solvents of variable F/Cl atomic ratio.

Table 2 shows that, at constant current density, the size of metallic grains is controlled by the F/Cl atomic ratio: the lower the content of free F⁻ anions in the melt, the finer the titanium powder. Thus, through the parameter F/Cl, it is possible to control the electrodeposition such that the resulting powder can be directly processed by powder metallurgy.

It has already been shown [10] that the electro-refining of titanium ensures an advanced purification of the metal: contamination with foreign cations drops below 10⁻³%. In addition the oxygen and nitrogen content must be strictly controlled, because this is decisive for further processing of the titanium powders. As this gaseous contamination may occur only at metal–melt or metal–gas boundaries it is obvious that its degree is directly dependent on the specific surface and implicitly, the apparent diameter of the metal particles. Table 3 supports this statement: the oxygen content doubles when the particle size decreases from 0.8 to 0.065 mm. Taking account of the data in Table 2, a direct dependence of oxygen content on the parameter F/Cl is also expected. Indeed the results listed in Table 4 show a systematic diminishing of oxygen content in the electrodeposited titanium as the F/Cl atomic ratio increases.

Table 4. Oxygen and nitrogen content in electrodeposited titanium in various solvent salt mixtures

Solvent composition/mol %	F/Cl ratio	Impurities/wt %	
		O_2	N_2
NaCl–KCl 50.0 : 50.0	0	0.080	0.001
NaCl–KCl–NaF 47.9 : 47.9 : 4.2	0.008	0.064	0.001
NaCl–KCl–NaF 46.4 : 46.4 : 7.2	0.041	0.060	0.006
NaCl–KCl–NaF 43.1 : 43.1 : 13.8	0.085	0.045	0.006
NaCl–KCl–NaF 40.4 : 40.4 : 19.2	0.126	0.045	0.006
LiF–NaF–KF 46.4 : 11.6 : 42.0	∞	0.043	0.007
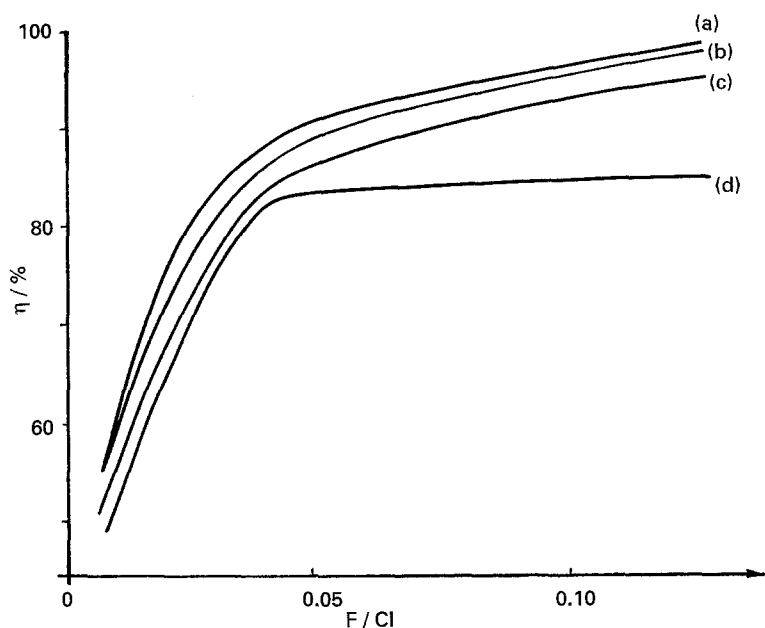
Fig. 8. η against F/Cl in NaCl–KCl–NaF solvent mixtures at different current densities: (a) 0.5×10^4, (b) 1×10^4, (c) 2×10^4 and (d) $3 \times 10^4 \, A\,m^{-2}$.

Considering all the results in Tables 2–4 it is clear that the free F^- ion content in the electrolyte requires careful control.

3.3. The influence of F/Cl atomic ratio on the current efficiency

Because the current efficiency, η, is obviously the basic criterion in the industrial application of any electrolytic process, the systematic investigation of its dependence on the F/Cl atomic ratio was also carried out. The results obtained with NaCl–KCl–NaF solvents are shown in Fig. 8; it is clear that η is higher the larger F/Cl (i.e. when the growth of well shaped dendrites is favoured). Moreover, because of the pronounced decline of η, concentrations below 10% NaF are not recommended. This result should be accepted with caution. Because this decrease can not be attributed to the cathodic process as such, it may suggest that special precautions must be taken in the recovery of the fine powders obtained at low values of the F/Cl atomic ratio (see Table 2).

References

[1]   F. R. Clayton, G. Mamantov and D. L. Maning, *J. Electrochem. Soc.* **120** (1973) 1193.
[2]   J. de Lepinay and P. Paillere, *Electrochim. Acta* **29** (1984) 1243.
[3]   J. de Lepinay, J. Bouteillon and M. J. Barbier, *J. Appl. Electrochem.* **17** (1987) 294.
[4]   A. Robin, J. de Lepinay, M. J. Brbier, *J. Electrochem. Soc.* **125** (1987) 230.
[5]   L. P. Polyakova, *Electrochim. Acta* **31** (1986) 159.
[6]   Y. Qi-qin, *Rare Metals of China* **1** (1982) 38.
[7]   J. G. Wurm, L. Gravel, R. J. A. Potvin, *J. Electrochem. Soc.* **104** (1957) 301.
[8]   N. F. H. Bright and J. G. Wurm, *Can. J. Chem.* **36** (1958) 1615.
[9]   A. Robin and J. de Lepinay, *Electrochim. Acta* **36** (1991) 1009.
[10] N. Ene and S. Zuca, *Rev. Roumaine Chim.* **36** (1991) 1238.
[11] S. Zuca and N. Ene, *Material Science Forum* **73–75** (1991) 643.
[12] N. Ene, PhD. thesis, Bucharest (1991).
[13] G. Brauer (ed.), 'Handbook of preparative inorganic chemistry', Vol. 2, 2nd edn, Academic Press, New York (1965) p. 1163.
[14] A. Calusaru, 'Electrodeposition of metal powders', Elsevier, Oxford (1979) p. 87.
[15] G. W. Mellors and S. Senderoff, *J. Electrochem. Soc.* **112** (1965) 266.
[16] J. Lumsden, 'Thermodynamics of molten salts', Academic Press, London (1966) p. 70.
[17] B. J. Fortin, *J. Electrochem. Soc.* **106** (1959) 428.
[18] M. V. Smironov, *Izd. Sibir. Otd. Akad. Nauk. SSSR* **10** (1959) 74.
[19] G. Mamantov, *J. Electroanal. Chem.* **9** (1965) 253.
[20] Cheng Guang-Sen, M. Okido and T. Oki, *J. Appl. Electrochem.* **17** (1987) 849.
[21] C. A. C. Sequeira, *J. Electroanal. Chem.* **23** (1988) 203.
[22] V. V. Nerubaschenko, *Fiz. Khim. Elektrochim. Rasplavi Tverd. Electroliti* **2** (1979) 65.
[23] J. Heyrovsky and D. Ilkovic, *Collection* **7** (1935) 198.
[24] V. I. Taranenko, I. V. Zarutskii, V. I. Shapaval, M. Makyta and K. Matiasovskiy, *Electrochim. Acta* **37** (1992) 263.